

## Deterministic Model of Multipath Fading for Circular and Parabolic Reflector Patterns

Dwight K. Hutchenson  
*dhutche@clemson.edu*

Daniel L. Noneaker  
*danno@ces.clemson.edu*

*Milton W. Holcombe Department of Electrical and Computer Engineering  
Clemson University*

### Abstract

*Traditionally, a probabilistic model has been used to analyze a wireless communication system's susceptibility to multipath fading. However, the characteristics of fading in an actual wireless communication link depend on the particular deterministic geometry of reflectors that the signal encounters. In this paper, we present a deterministic model of multipath propagation, and we apply the model to two reflector geometries: a circular pattern of reflectors and a parabolic pattern of reflectors. Numerical results for each case are included, and it is shown that the geometry of the reflectors that the signal encounters has a substantial effect on the rate of change in signal strength observed by a mobile receiver.*

### 1. Introduction

In a wireless mobile communication system, the received signal is made up of components traveling over multiple propagation paths of differing length, often with no line-of-sight component. The signal components do not arrive at the receiver in phase with one another, in general, and the relative phase angles and amplitudes of the components at the receiver determine the overall strength of the received signal. If the receiver changes locations, the phase relationship among the reflected signal components changes, and hence, the strength of the received signal varies. This phenomenon is referred to as *multipath fading*, and it results in a signal strength at the receiver that is a function of its position. Position-dependent signal strength results in time-dependent signal strength if the transmitter, receiver, or reflectors are in motion.

Analyses of communication-system performance in multipath fading typically employ a statistical model of the fading observed at the receiver. The most commonly used models fall within the class of Gaussian wide-sense stationary uncorrelated scattering (GWSSUS) channels introduced in [1]. One popular GWSSUS channel is the so-called Jakes-Clarke model [2] which exhibits the long

time-correlation tails that are often observed in field measurements of cellular communication systems. Another GWSSUS channel with an exponential time-correlation function [3] is equivalent to a Gauss-Markov channel, and it is also widely used in system performance analysis. These statistical models are favored for use in Monte Carlo simulation of communication systems because the models are amenable to efficient software implementation and because they provide common benchmarks for system designs. (The Gauss-Markov channel has a particularly simple algorithmic implementation.)

The relationship of the statistical models to actual propagation environments that are encountered in practice is problematic, however. The Jakes-Clarke model is based on a circular array of infinitesimal reflectors and independent random phase shifts of the reflected signal components. Many other GWSSUS models, such as the Gauss-Markov model, are not easily related to any physical configuration of reflectors. In this paper we examine the effect that the physical configuration of reflectors has on the empirical fading characteristics observed at the receiver. From this we gain insight into the extent to which the properties of the channel may deviate from those predicted by the use of a single statistical model.

In this paper, a model is presented for the strength of a single-frequency signal at the receiver as a function of the receiver's position in a deterministic multipath environment. The model is applied to two reflector geometries: a circular reflector pattern and a parabolic reflector pattern. The fading characteristics are considered for the two reflector geometries for a choice of model parameters that allow for a fair comparison between them. It is shown that there are substantial differences in the fading that results from the two reflector geometries. Specifically, there is a greater fluctuation in the signal strength over the same area with a circular reflector pattern than with a parabolic reflector pattern of similar dimensions. Thus the fading characteristics of a mobile receiver of a given velocity is shown to depend significantly on the particular reflector geometry.

## 2. Development of the Model

In this model, a given reflector pattern is considered and used to determine the strength of a single-frequency signal as a function of receiver position. Let  $\omega_c$  be the frequency of the signal in radians per second. Because this is the only frequency at which energy is present in the signal, the time-domain expression for the signal received at a point,  $S$ , in the  $x$ - $y$  plane, can be written in the form:

$$\mathcal{E}_S(t) = E \cos(\omega_c t + \phi_S). \quad (1)$$

Alternatively, it can be written the form:

$$\mathcal{E}_S(t) = \text{Re}\{E_S e^{j\omega_c t}\}, \quad (2)$$

where

$$E_S = E e^{j\phi_S} \quad (3)$$

is the baseband-equivalent complex representation of the signal.

The signal received at  $S$  can also be written as a sum of the components traveling along each reflective path from the transmitter to the receiver at  $S$ :

$$E_S = E_0 + E_1 + \dots + E_{n-1} + E_n + \dots \quad (4)$$

Suppose the multipath component with complex amplitude  $E_0$  is chosen as the reference component. Then the complex amplitude of any other multipath component can be expressed in terms of  $E_0$ . Let  $k=2\pi f d/c$  denote the free-space phase constant and  $\Delta_n$  denote the difference in the path propagation distances of components  $E_n$  and  $E_0$ . Then the signal component  $E_n$  can be written as

$$E_n = E_0 e^{-jk\Delta_n}. \quad (5)$$

In general, an expression for the signal at the receiver is obtained by summing all of the signal components expressed in the form of equation (5).

### 2.1. Circular Reflector Pattern

The scenario for the circular reflector pattern consists of a transmitter at a point  $Q$  in the  $x$ - $y$  plane on the negative  $x$ -axis, which is at a distance  $q > 0$  from the origin,  $O$ . The reference reflector is positioned at  $P_0$ , which has a distance  $r > 0$  from the origin and is on the negative  $x$ -axis. Another reflector is positioned at  $P_n$ , which also has a distance  $r > 0$  from the origin, but is on a line at an angle  $\theta_n$  with the negative  $x$ -axis. The receiver is located at  $S$ , which is on a line at an angle  $\eta$  with the positive  $x$ -axis, at a distance of  $\rho \geq 0$  from the origin.

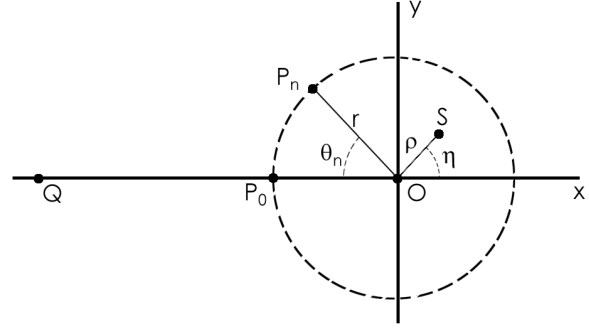


Figure 1. Circular reflector pattern

In order for the signal component  $E_n$  to be expressed in the form shown in equation (5), the phase shift  $\Delta_n$  of  $E_n$  relative to  $E_0$  must be found. It is assumed that the distance from the transmitter to the origin is much larger than the distance from any reflector to the origin ( $q \gg r$ ). It is also assumed that the distance between any reflector and the origin is much larger than the distance between the receiver and the origin ( $r \gg \rho$ ). Under these assumptions, accurate first-order approximations result in

$$\Delta_n = r(1 - \cos \theta_n) + \rho \cos(\theta_n + \eta). \quad (6)$$

Therefore, if  $N$  reflectors are uniformly distributed around the circle centered at the origin with radius  $r$ , the signal received at  $S$  can be written as

$$E_S = E_0 \sum_{n=0}^{N-1} e^{-jk(r(1 - \cos \theta_n) + \rho \cos(\theta_n + \eta))}. \quad (7)$$

If equation (7) is normalized by  $N$  and  $N$  is allowed to approach infinity we obtain:

$$E_S = \frac{E_0}{2\pi} \int_0^{2\pi} e^{-jk(r(1 - \cos \theta) + \rho \cos(\theta + \eta))} d\theta. \quad (8)$$

By manipulating terms and using an expression for the Bessel function [4], equation (8) can be simplified once more to obtain the model equation for the received signal at point  $S$  due to an infinitely populated circular pattern of reflectors:

$$E_S = E_0 e^{-jkr} J_0 \left( k \sqrt{r^2 + \rho^2 + 2r\rho \cos \eta} \right) \quad (9)$$

where  $J_0$  is the Bessel function of the first kind of zero order.

### 2.2. Parabolic Reflector Pattern

The scenario for the parabolic reflector pattern consists of a transmitter at a point  $Q$  in the  $x$ - $y$  plane on the negative  $x$ -axis, which is at a distance  $q > 0$  from the origin,  $O$ . The reflectors in this scenario populate a portion of a parabola described by the equations  $x = g(y) = ay^2 - h$  ( $a$  and  $h$  are positive constants) and  $y_{min} \leq y \leq$

$y_{max}$ . The reference reflector is located at the vertex of the parabola, and this point is denoted  $P_0$ . Another reflector is located at point  $P_n$  with coordinates  $(g(y_n), y_n)$ . The receiver is located at point  $S$ , which has coordinates  $(S_x, S_y)$ . Again we consider the case in which the distance from the transmitter to the origin is much greater than the distance from any reflector to the origin.

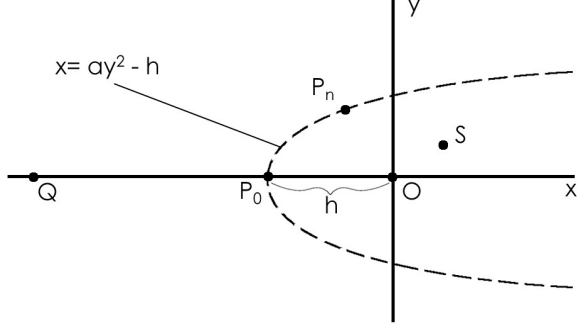


**Figure 2. Parabolic reflector pattern**

In the case of the circular reflector pattern, the expression for uniform placement of reflectors around the circle permits an analysis for the limiting case of a continuum of reflectors with uniform reflected signal density around the circle. A similar approach could be used for the parabolic reflector pattern, but it results in analytical difficulties. Instead an expression is developed for reflectors that are placed on the parabola at fixed intervals with respect to the  $y$ -axis coordinate. The received signal at reflector  $P_n$  is weighted by the arc length of the parabola between  $P_{n-1}$  and  $P_n$ . This corresponds to a uniform reflected signal density along the parabola in the limit as the number of reflectors approaches infinity.

Another key difference in the development of the model for the parabolic reflector pattern versus that of the circular reflector pattern is the consideration of signal strength attenuation with distance. Because the receiver is near the center of the circle in the circular reflector pattern case, all multipath components arriving at the receiver have approximately the same strength. This is not true in the case of the parabolic reflector pattern. Therefore, a multiplicative path-loss term must be introduced in the complex amplitude of each received signal component to account for its position-dependent attenuation. This term

is of the form  $\frac{1}{\{r(y)\}^\zeta}$  where  $r(y)$  is the distance from

the reflector and  $\zeta$  is the exponential path-loss parameter. Because a two-dimensional spatial model is considered in this development, a natural choice for this parameter is  $\zeta = 1/2$ .

Let  $E(y_n)$  represent the signal component reflected at  $P_n$ . For closely spaced reflectors, the arc length along the parabola between  $P_{n-1}$  and  $P_n$  is closely approximated by the distance between  $P_{n-1}$  and  $P_n$ . By the mean-value theorem there exists  $y_n^*$ ,  $y_{n-1} \leq y_n^* \leq y_n$  such that the distance between  $P_n$  and  $P_{n-1}$  can be written as

$$\overline{P_n P_{n-1}} = \sqrt{1 + g'(y_n^*)^2} (y_n - y_{n-1}). \quad (10)$$

Thus for large  $N$  the received signal is given by:

$$E_S = \sum_{n=1}^N \frac{E(y_n^*) \sqrt{1 + g'(y_n^*)^2}}{\{r(y_n^*)\}^\zeta} (y_n - y_{n-1}). \quad (11)$$

As the number of reflectors approaches infinity, the received signal, normalized by  $N$ , becomes a definite integral, given by

$$E_S = \int_{y_{min}}^{y_{max}} \frac{E(y) \sqrt{1 + g'(y)^2}}{\{r(y)\}^\zeta} dy. \quad (12)$$

The expression for the signal component  $E(y)$  is developed in a similar manner as the expression for  $E_n$  is developed in the circular reflector pattern case by finding the extra distance that component  $E(y)$  travels in relation to the distance traveled by a reference signal,  $E_0 = E(0)$ . Some first-order approximations are used in the development to simplify the expression.

The model for the received signal for the parabolic reflector pattern case is determined to be

$$E_S = \int_{y_{min}}^{y_{max}} \frac{E(y) \sqrt{1 + (2ay)^2}}{\{r(y)\}^\zeta} dy \quad (13)$$

where

$$E(y) = E_0 e^{-jk \left[ (ay^2 - h + \sqrt{(ay^2 - h)^2 + y^2}) + \frac{(-ay^2 + h)S_x - yS_y}{\sqrt{(ay^2 - h)^2 + y^2}} \right]} \quad (14)$$

and

$$r(y) = \sqrt{(ay^2 - h - S_x)^2 + (y - S_y)^2}. \quad (15)$$

### 3. Numerical Results

Numerical values are chosen for the parameters in the circular and parabolic reflector pattern models to permit a fair comparison of their fading characteristics. A comparison of the fading characteristics for one set of parameters is detailed below. This set of parameters provides a fair comparison between the two reflector patterns, because the distance from the receiver to the nearest reflector is similar for each case. For both models, the units of distance and the  $x$  and  $y$  coordinates on the plots are given in terms of the signal's wavelength.

Hence, the free-space constant used is  $k=2\pi/\lambda=2\pi$ . Also, the complex constant,  $E_0$ , is chosen to equal 1 in both models.

For the circular reflector pattern, the radius of the circular pattern is chosen to be ten wavelengths. Recall that the parabolic reflector pattern is described by the equation,  $x = ay^2 - h$ . In order for the distance from the receiver to the nearest reflector to be similar for both reflector patterns, the parameters  $a$  and  $h$  are chosen such that the parabolic reflector pattern will cross the  $-x$ ,  $+y$ , and  $-y$  axes at the same points as the circular reflector pattern. Therefore these parameters are chosen as  $a=0.1$  and  $h=10$ . The parabola's truncation is specified by  $y_{max} = -y_{min} = 20$ . Since approximations are used in the development of the models that the distance from the origin to the receiver is much smaller than the distance from the origin to any reflector, signal strengths are calculated for receiver locations at  $-2 \leq x \leq 2$  and  $-2 \leq y \leq 2$ . Figure 3 shows both reflector patterns and the area over which receiver locations are considered.

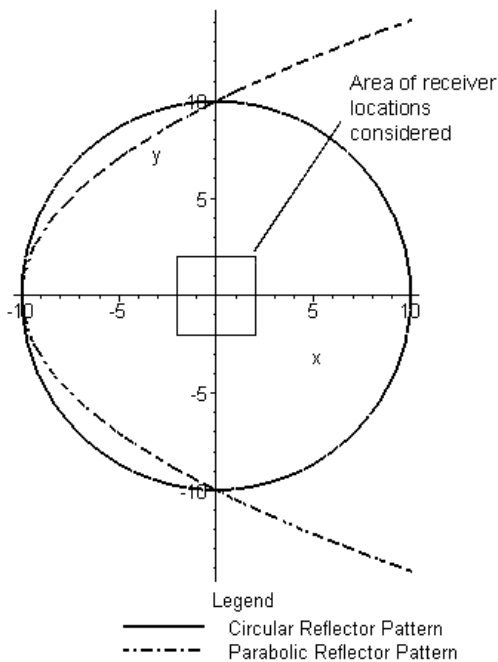


**Figure 3. Reflector patterns for numerical analysis**

Signal strengths are calculated for each reflector pattern for uniformly distributed receiver locations within the chosen area. All figures show results for 441 sample locations except Figures 6 and 7, which show results for 10,000 sample locations within the same area. Figure 4 (a) shows a plot generated from the data from the circular model. The magnitude of the received signal at a receiver location  $(x, y)$ , is displayed as the corresponding  $z$ -coordinate (axis labeled  $|E_S|$ ). Figure 4 (b) shows the same

plot from a top view. Darker shading corresponds to a smaller signal strength. Figures 5(a) and 5(b) show similar plots for the case of the parabolic reflector pattern.

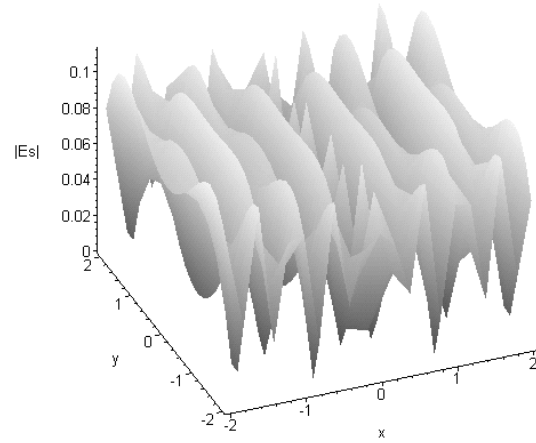


**Figure 4(a). Signal strength for circular reflector pattern model**

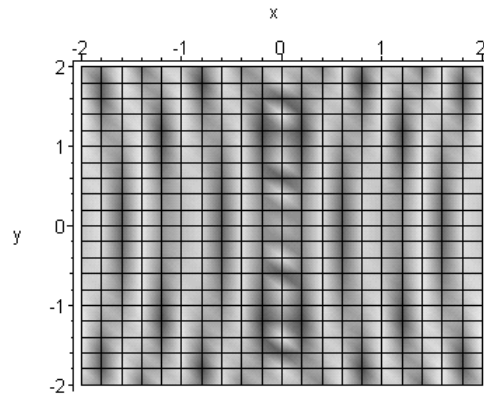


**Figure 4(b). Signal strength for circular reflector pattern model (top view)**

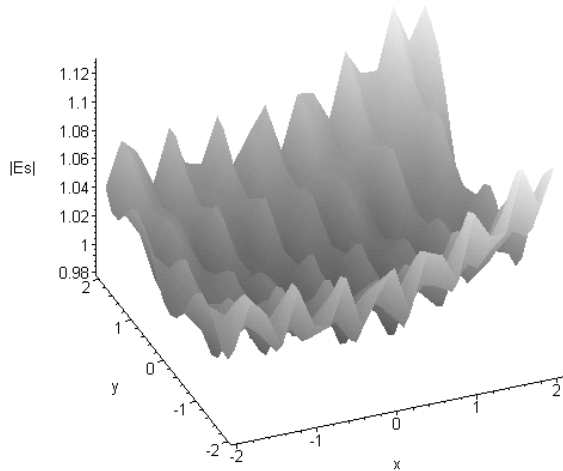


**Figure 5(a). Signal strength for parabolic reflector pattern model**

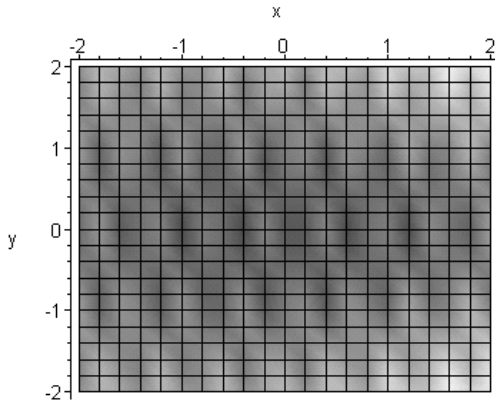


**Figure 5(b). Signal strength for parabolic reflector pattern model (top view)**

The bar graphs of Figures 6 and 7 show the empirical probability distribution function and probability density function, respectively, of the signal magnitudes for the case of the circular reflector. Figures 8 and 9 show the empirical probability distribution function and probability density function of the signal magnitudes for the parabolic reflector case.

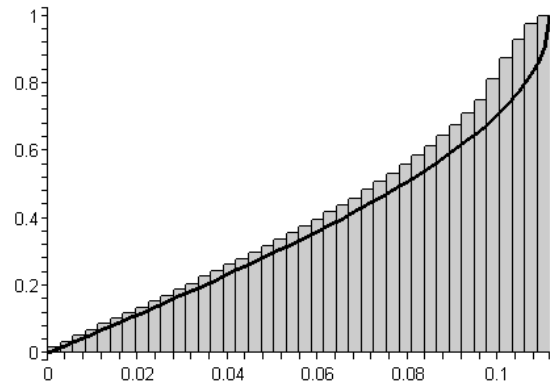


**Figure 6. Probability distribution function of signal strength for circular reflector pattern model**

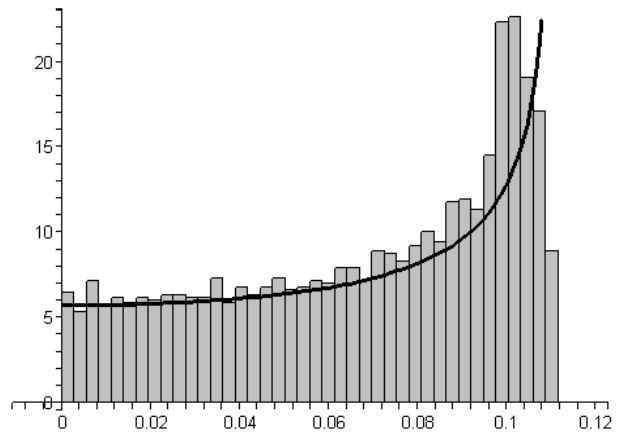


**Figure 7. Probability density function of signal strength for circular reflector pattern model**

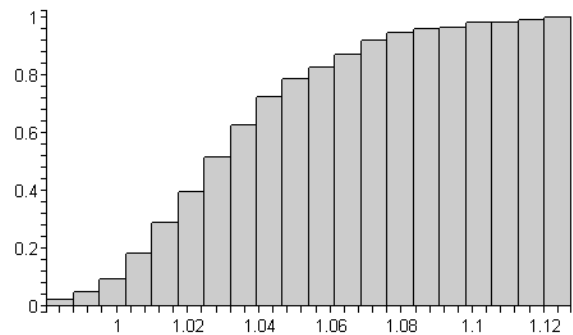


**Figure 8. Probability distribution function of signal strength for parabolic reflector pattern model**

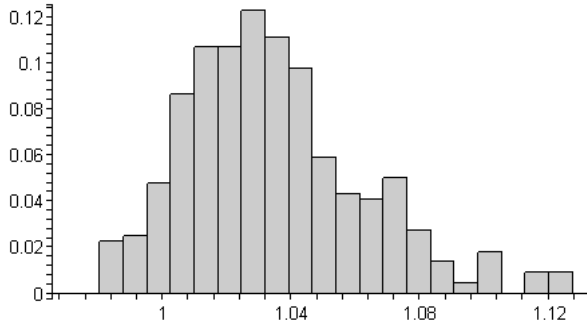


**Figure 9. Probability density function of signal strength for parabolic reflector pattern model**

For the circular reflector pattern, the minimum and maximum signal magnitudes for receiver locations over the chosen area are  $5.907 \cdot 10^{-4}$  and 0.1116, respectively. Therefore, the signal strength fluctuates by 99.47% of its maximum value. For the parabolic reflector pattern, in contrast, the minimum and maximum signal magnitudes are 0.9805 and 1.1275, respectively. This means the signal strength only fluctuates by 13.04% of its maximum value. Thus the receiver observes much less spatial variation in the signal strength (and much less severe fading) as it moves near the origin if the reflector pattern is parabolic rather than circular.

The probability distribution function and probability density function for signal magnitudes at the receiver can also be derived analytically for the case of the circular reflector pattern under the conditions we consider. Let the random variable  $Z$  represent the received signal strength at a randomly selected location near the origin. It can be shown that in the limit as  $q \gg r$ , and  $r \gg \rho$ , the probability distribution function and probability density function of  $Z$  are

$$F_Z(z) = \begin{cases} 0 & z < 0 \\ \frac{2}{\pi} \arcsin\left(\frac{z}{\alpha}\right) & 0 \leq z \leq \alpha, \\ 1 & z > \alpha \end{cases}, \quad (16)$$

and

$$f_Z(z) = \begin{cases} 0 & z < 0 \\ \left( \alpha \pi \sqrt{1 - \left(\frac{z}{\alpha}\right)^2} \right)^{-1} & 0 \leq z \leq \alpha, \\ 0 & z > \alpha \end{cases}, \quad (17)$$

respectively, where  $\alpha$  represents the greatest signal strength observed. The probability distribution function in equation (16) is plotted in Figure 6 as the solid black line. A similar plot is shown in Figure 7 for the probability

density function in equation (17). Note that both asymptotic analytical results yield close agreement with the empirical results of our example.

#### 4. Conclusion

In this paper we present a model for the strength of a single-frequency signal at a receiver in the presence of multipath propagation. A deterministic reflector pattern is modeled, and the model is used to determine the strength of the signal at the receiver as a function of the receiver's position. Signal-strength expressions are developed for general circular and parabolic reflector patterns. Examples of both reflector patterns are considered, using parameters for each which permit a fair comparison of their fading characteristics. The parabolic reflector pattern is found to produce substantially less variation in the signal strength as a function of receiver position than the circular reflector pattern. This illustrates that the fading characteristics depend significantly on the physical configuration of the reflectors, and it highlights the drawbacks associated with using a single statistical model to predict fading channel properties.

#### 5. Acknowledgements

This work was supported in part by the National Science Foundation under grant EEC-0097557 and in part by the U.S. Army Research Laboratory and the U.S. Army Research Office under grant DAAD-19-00-0156.

#### 6. References

- [1] P. A. Bello, "Characterization of randomly time variant linear channels," *IEEE Trans. Commun. Syst.*, vol CS-11, pp. 360-393, Dec. 1963.
- [2] R. H. Clarke, "A statistical theory of mobile-radio reception," *Bell Syst. Tech. J.*, vol. 47, no. 4, pp. 957-1000, July-Aug. 1968.
- [3] P. A. Bello and B. D. Nelin, "The influence of fading spectrum on the binary error probabilities of incoherent and differentially coherent match filter receivers," *IRE Trans. Commun. Syst.*, vol CS-10, pp. 16-168, June 1962.
- [4] F. Bowman, *Introduction to Bessel Functions*, Dover Publications, March 1968